International Journal of Electrical, Electronic and Communication Sciences
ISSN: 2517-9438
Vol:4, No:3, 2010

# Solution of Optimal Reactive Power Flow using Biogeography-Based Optimization

Aniruddha Bhattacharya, *Member, IEEE,* and Pranab Kumar Chattopadhyay

*Abstract*—Optimal reactive power flow is an optimization problem with one or more objective of minimizing the active power losses for fixed generation schedule. The control variables are generator bus voltages, transformer tap settings and reactive power output of the compensating devices placed on different bus bars. Biogeography-Based Optimization (BBO) technique has been applied to solve different kinds of optimal reactive power flow problems subject to operational constraints like power balance constraint, line flow and bus voltages limits etc. BBO searches for the global optimum mainly through two steps: Migration and Mutation. In the present work, BBO has been applied to solve the optimal reactive power flow problems on IEEE 30-bus and standard IEEE 57-bus power systems for minimization of active power loss. The superiority of the proposed method has been demonstrated. Considering the quality of the solution obtained, the proposed method seems to be a promising one for solving these problems.

*Keywords*—Active Power Loss, Biogeography-Based Optimization, Migration, Mutation, Optimal Reactive Power Flow.

## I. Introduction

OPTIMAL Reactive Power Flow (ORPF) is an important tool for power system operators both in planning and operating stages. It has a significant influence on the economic and secure operation of power systems and may be considered as a sub-set of the more general power system problem known as optimal power flow (OPF) problem. The active power loss, voltage profile and voltage security in a power system strongly depend upon the flow of reactive power in the transmission lines. The ORPF deals with control of generator voltages, transformer tap ratio, and reactive power compensating devices (shunt capacitors). All these variables strongly affect the flow of the reactive power in the system. Some additional constraints like reactive power capability of generators, voltage magnitude limits of load bus etc should also be observed to obtain a viable solution. The main objective of an ORPF program is to minimize the system active power loss. But minimization of active power loss of power system may result in such settings of the control variables which might cause unattractive voltage profile and voltage stability margin at different bus bars. In such situations, sometimes it is sensible to consider voltage profile improvement and voltage stability limit enhancement as part of objective of ORPF problems. Voltage stability margin can be enhanced by properly controlling and relocating reactive power generations. In case the reactive power generation capacity of a system is very close to its reactive power demand then installation of few extra reactive power sources at some suitable points in the system may improve the voltage profile, voltage stability margin along with reduction of active power loss of the system. Optimal reactive power flow problem has been rigorously studied over the past few decades. Many optimization techniques have emerged so far and have been applied to solve the problem. The earlier ORPF algorithms were based on classical mathematical programming methods. Nonlinear programming (NLP) [1], Linear programming (LP) [2-3] Quadratic programming (QP) [4], Newton-based method [5], interior point methods (IPM) [6], [7], mixed integer programming [8], decomposition approach [9], dynamic programming [10] have successfully proved their capabilities in this field. But today's ORPF problem is not a mathematically convex problem; as a result most of the classical optimization techniques might converge to a local optimum instead of at the global optimum. Moreover, these classical techniques can not solve the complex objective functions which are not differentiable, particularly in large dimension problems or with complicated constraints. Due to significant improvement in the capability of computers in recent years, evolutionary algorithms (EAs), such as genetic algorithm (GA) [11-15], evolutionary programming (EP) [16-17], particle swarm optimization (PSO) [18-24] and differential evolution (DE) [25-28] are being applied for solving various reactive power flow related problems to overcome some of the drawbacks of conventional techniques. Genetic algorithm (GA) has been applied successfully in different reactive power optimization problems. K. Iba et al. [11] proposed an integer/float mixed coding GA to reduce the system loss. K. Y. Lee et al. [12] presented an improved version of Genetic Algorithm after incorporating a new population selection and generation method within simple genetic algorithm to find the optimal placement and size of VAR compensating devices. An adaptive genetic algorithm (AGA) is proposed by Q.H. Wu et al. [13], for optimal reactive power dispatch problems and voltage control operation. Here, the probabilities of crossover and mutation are varied within basic GA, depending on the fitness values of the solutions to prevent premature convergence and refine the convergence performance of genetic algorithms. For the optimization of reactive power, for improvement of voltage profiles and minimization of real power loss, G. A. Bakare et al. [14] proposed a micro-genetic based approach. W. Yan et. al. [15] presented a novel hybrid method for the optimal reactive power flow problems after integrating genetic algorithm (GA) with nonlinear interior point method (IPM). Evolutionary Programming (EP) has been applied successfully in different power system optimization problems. In 1995, Q.H. Wu et al. [16] applied this technique for reactive power

A. Bhattacharya is a Ph.D scholar at Jadavpur University, Kolkata, West Bengal, 700 032 INDIA e-mail: (bhatta.aniruddha@gmail.com).
Prof. P. K. Chattopadhyay is with the Department of Electrical Engineering, Jadavpur University, Kolkata, West Bengal 700 032 INDIA .

dispatch and voltage control of power systems. Later on in 1997, an evolutionary programming technique for optimal reactive power planning and minimization of active power loss was proposed by the same authors [17]. Particle swarm optimization (PSO) has also a wide range of application in power system ORPF problems. H. Yoshida et al. [18] applied PSO for reactive power and voltage control with voltage security assessment. W. Zhang et al. [19] developed an adaptive PSO for reactive power optimization. B. Zhao et al. [20] presented multi-agent-based PSO method in reactive power dispatch problem. A. A. A. Esmin et al. [21] proposed a hybrid PSO with mutation operator to minimize the active power loss. M. S. Kumari et al. [22] solved optimal reactive power control problem using an improved version of PSO. For control of reactive power and voltage, J. G. Vlachogiannis et al. [23] proposed new PSO algorithms. Cai et al. [24] presented a modified version of PSO method for solution of optimal reactive power dispatch problems along with improvement in voltage stability margin. C. H. Liang et al. [25] applied differential evolution (DE) successfully for active power loss minimization of IEEE 14, 30, 57 and 118-bus systems. In 2007, G. A. Bakare et al. [26] proposed differential evolution (DE) for mixed integer, non-linear reactive power optimization problems. M. Varadarajan et al. [27] presented application of differential evolution for both network loss minimization and voltage security problems. C.Y. Chung et al. [28] proposed a hybrid algorithm of DE and EP for optimal reactive power flow problem to minimize active power loss of power system. Another new population-based heuristic search algorithm known as Seeker optimization algorithm (SOA) has been developed and applied effectively for reactive power dispatch problems to minimize active power loss [29]. Recently, a new concept, based on Biogeography-Based Optimization (BBO) [30], has been proposed by Dan Simon. BBO is based on the two fundamental mechanisms, e.g., Migration and Mutation. Like GAs and PSO, BBO has a way of sharing information between solutions. GA solutions "die" at the end of each generation, while PSO and BBO solutions survive forever. PSO solutions are more likely to clump together in similar groups, while GA and BBO solutions do not have any built-in tendency to cluster. Again in BBO poor solutions accept a lot of new features from good ones. The additions of new features to low quality solutions may improve the quality of those solutions. BBO has already been applied successfully to solve non-convex, large, complex Economic Load Dispatch problems [31]. These versatile properties of this new algorithm encouraged the authors to apply this newly developed algorithm to solve ORPF problems for minimization of active power loss. The performance of the proposed method has been tested on IEEE 30-bus and IEEE 57-bus systems. It has been found through extensive experimentations that performance of the proposed method is better in both the cases, compared to Seeker Optimization Algorithm (SOA) [29], different PSO [29], DE [26] and other techniques. Section II of the paper provides a brief description and mathematical formulation of optimal reactive power flow (ORPF) problems. The original BBO approach is described in Section III along with a short description of the algorithm. The simulation studies are discussed in Section IV. The conclusion is drawn in Section V.

## II. ORPF PROBLEM FORMULATION

The optimal reactive power flow (ORPF) problem is mainly concerned with minimization active power loss of power system, subject to various equality and inequality constraints. Mathematically ORPF problem may be represented as

$$Min\ J(x,u) \tag{1}$$

$$Subject\ to\ g(x,u)=0 \tag{2}$$

$$and\ h(x,u)<=0 \tag{3}$$

Where, *J* is the objective function to be minimized. For loss minimization problem, $J$ can be defined as follows:

$$J=P_{loss}=\sum_{k\in NTL} g_k(V_i^2+V_j^2-2V_iV_jcos\theta_{ij}) \tag{4}$$

Here, $P_{loss}$ denotes active power loss of the power system; $NTL$ is the number of network branches; $g_k$ is the conductance of branch $k$; $k=(i,j)$, $i\in NB$, $j\in N_i$ ; $NB$ is the total number of bus; $N_i$ is the set of number of bus adjacent to bus $i$; $\theta_{ij}$ is the voltage angle difference between bus $i$ and $j$; $V_i$ and $V_j$ are the voltage of bus $i$ and $j$ respectively. *x* and *u* are the vectors of dependent and control variables respectively. The vector of dependent variables *x* may be represented as

$$x^T=[P_{G1},V_{L1}.....V_{LNPQ},Q_{G1}.....Q_{GNPV}] \tag{5}$$

where, $P_{G1}$ denotes the slack bus power; $V_L$ is the ***PQ*** bus voltages; $Q_G$ is the reactive power output of the generators; $NPV$ is the number of voltage controlled bus; $NPQ$ is the number of ***PQ*** bus. The vector of control variables may be written as

$$u^T=[V_{G1}.....V_{GPV},T_1.....T_{NT},Q_{C1}.....Q_{CNC}] \tag{6}$$

where, ***NT*** and ***NC*** are the number of tap changing transformers and shunt $VAR$ compensators respectively, $V_G$ is the terminal voltages at the voltage controlled bus, ***T*** is the tap ratio of the tap changing transformers and $Q_C$ is the output of shunt $VAR$ compensators.

Here, *g* is the set of equality constraints representing the following load flow equations:

$$P_{Gi}-P_{Di}=V_i\sum_{i=1}^{NB}V_k(G_{ik}cos\theta_{ik}+B_{ik}sin\theta_{ik}) \tag{7}$$

where i=1,2.....NB

$$Q_{Gi}-Q_{Di}=V_i\sum_{i=1}^{NB}V_k(G_{ik}sin\theta_{ik}+B_{ik}cos\theta_{ik}) \tag{8}$$

where i=1,2.....NB

where,$P_{Gi}$ and $Q_{Gi}$ are the injected active and reactive power, $P_{Di}$ and $Q_{Di}$ are the active and reactive power demand at bus *i*; $G_{ik}$ and $B_{ik}$ are the transfer conductance and susceptance between bus *i* and *k*, $\theta_{ik}$ is the phase angle difference between the voltages at bus *i* and *k*. *h* is the set of system operating constraints which include:

### A. Generator Constraints

For all Generators, including the slack, the voltages and reactive power outputs must be restricted within their permissible lower and upper limits as follows:

$$V_{Gi}^{min} \leq V_{Gi} \leq V_{Gi}^{max}, i = 1, 2, ...NPV \tag{9}$$

$$Q_{Gi}^{min} \leq Q_{Gi} \leq Q_{Gi}^{max}, i = 1, 2, ...NPV \tag{10}$$

### B. Transformer Constraints

Transformer tap settings must be within its specified lower and upper limits as follows:

$$T_i^{min} \leq T_i \leq T_i^{max}, i = 1, 2, ...NT \tag{11}$$

### C. Shunt VAR Compensator Constraints

Reactive power output of shunt $VAR$ compensators must be restricted within their lower and upper limits as follows:

$$Q_{ci}^{min} \leq Q_{ci} \leq Q_{ci}^{max}, i = 1, 2, ...NC \tag{12}$$

### D. Voltage Constraint

Voltage of each PQ bus must be within its lower and upper operating limits as follows:

$$V_{Li}^{min} \leq V_{Li} \leq V_{Li}^{max}, i = 1, 2, ...NPQ \tag{13}$$

The inequality constraints of the dependant variable (like $P_{G1}$, $V_L$, $Q_G$) may be incorporated within the objective function as quadratic penalty terms in order to keep their final values close to their operating limits. Therefore, to account for these constraints, the objective function (1) may be modified to

$$J_{mod} = P_{loss} + \lambda_P (P_{G1} - P_{G1}^{lim})^2 + \lambda_V \sum_{i=1}^{NPQ} (V_{Li} - V_{Li}^{lim})^2 + \lambda_Q \sum_{i=1}^{NPV+slack} (Q_{Gi} - Q_{Gi}^{lim})^2 \tag{14}$$

Where $\lambda_P$, $\lambda_V$, $\lambda_Q$ are the penalty factors. $V_{Li}^{lim}$ & $Q_{Gi}^{lim}$ are calculated as

$$V_{Li}^{lim} = \begin{cases} V_{Li}^{max}, & V_{Li} > V_{Li}^{max}; \\ V_{Li}^{min}, & V_{Li} > V_{Li}^{min}; \\ 0, & \text{else}; \end{cases} \tag{15}$$

$$Q_{Gi}^{lim} = \begin{cases} Q_{Gi}^{max}, & Q_{Gi} > Q_{Gi}^{max}; \\ Q_{Gi}^{min}, & Q_{Gi} > Q_{Gi}^{min}; \\ 0, & \text{else}; \end{cases} \tag{16}$$

## III. BIOGEOGRAPHY-BASED OPTIMIZATION

BBO [30] is a population based, stochastic optimization technique developed by Dan Simon in 2008, which is based on the concept of biogeography that deals with nature's way of distribution of species. Distribution of a species from one place to another is influenced by factors such as rainfall, diversity of vegetation, diversity of topographic features, land area, temperature etc. Areas, where these factors are highly favorable tend to have a larger number of species, compared with a less favorable area. Movement of species from one area to another area, facilitates sharing of their features with each other. Owing to this movement, the quality of some species may improve due to exchange of good features with better species. In context of biogeography, a habitat is defined as an Island (area) that is geographically isolated from other Islands. Geographical areas that are well suited as residences for biological species are said to have a high habitat suitability index (*HSI*). The variables that characterize habitability are called suitability index variables (*SIVs*). *SIVs* can be considered as the independent variables of the habitat and *HSI* calculation is carried out using these variables. The migration of some species from a habitat to an exterior habitat is known as emigration process and an entry into one habitat from an outside is known as immigration process. The rate of immigration and the emigration are functions of the number of species in the habitat. Habitats with a high *HSI* have a low species immigration rate as they are already saturated with species. As a result, these high *HSI* habitats are more static in their species distribution than low *HSI* habitats. On the contrary emigration rate of high *HSI* habitats are high. The large numbers of species on high *HSI* islands have many opportunities to emigrate into neighboring habitats having less number of species and share their characteristics with those habitats. For this reason habitats with a low *HSI* have a high species immigration rate. Figure 1 illustrates a model of species movement process in a single habitat with straight line immigration and emigration curves. This concept of biogeography has evolved a new optimization process, known as biogeography-based optimization (BBO) [30]. In biogeography-based optimization process,, a good solution is similar to an island with a high Habitat Suitability Index (*HSI*), and a poor solution is equivalent to an island with a low *HSI*. High *HSI* solutions resist change more than low *HSI* solutions and tend to share their features with low *HSI* solutions. (This does not mean that the superior features disappear from the high *HSI* solution; the shared features still remain in the high *HSI* solutions, while at the same time appearing as new features in the low *HSI* solutions.). In this way poor solutions accept a lot of new features from good solutions. This addition of good features to low *HSI* solutions may raise the quality of those solutions. Mathematically the concept of emigration and immigration is represented by a probabilistic model. If $P_s(t)$denotes the probability that a habitat contains exactly $S$ species at time $t$, at time $t + \Delta t$ the probability is

$$P_s(t + \Delta t) = P_s(t)(1 - \lambda_s \Delta t - \mu_s \Delta t) + P_{s-1}\lambda_{s-1}\Delta t + P_{s+1}\mu_{s+1}\Delta t \tag{17}$$

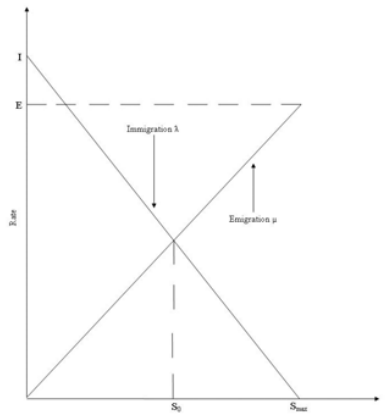


Fig. 1. Species model of a single habitat

where $\lambda_s$ and $\mu_s$ are the immigration and emigration rates when there are $S$ species in the habitat. If time $\Delta t$ is small enough so that the probability of more than one immigration or emigration can be ignored then taking the limit of equation (17) as $\Delta t \to 0$ gives the following equation

$$\dot{P}_s = \begin{cases} -(\lambda_s + \mu_s)P_s + P_{s+1}\mu_{s+1}; S = 0, \\ -(\lambda_s + \mu_s)P_s + P_{s+1}\mu_{s+1} + P_{s-1}\lambda_{s-1}; 1 \leq S \leq S_{max} - 1 \\ -(\lambda_s + \mu_s)P_s + P_{s-1}\lambda_{s-1}; S = S_{max}, \end{cases} \tag{18}$$

From the straight-line graph of figure 1, the equation for emigration rate $mu_k$ and immigration rate $lambda_k$ for *k* number of species is derived as per following way:

$$\mu_k = \frac{Ek}{n} \tag{19}$$

$$\lambda_k = I\left(1 - \frac{k}{n}\right) \tag{20}$$

where, *E* and *I* are the maximum emigration rate and maximum immigration rate respectively. *n* is the total number of species in the habitat.

When $E = I$

$$\lambda_k + \mu_k = E \tag{21}$$

BBO mainly works based on Migration and Mutation.

### A. Migration

With probability $P_{mod}$, known as Habitat Modification Probability each solution can be modified based on other solutions. If a given solution $S_i$ is selected to be modified, then its immigration rate $\lambda_i$ is used to probabilistically decide whether or not to modify any suitability index variable *(SIV)* in that solution. After selecting any *SIV* of that solution for modification, emigration rates $\mu_j$ of other solutions $S_j$ ($S_j$ is $j-th$ solution set other than $S_i$,i.e. $j \neq i$) are used to select which solutions among the population set will migrate randomly to chosen *SIVs* to the selected solution $S_i$.Details about the algorithm of migration are available in [30], [31].

### B. Mutation

In BBO species count probabilities $P_s$ are used to determine mutation rates. The probabilities of each species count can be calculated using the differential equation (18). Each habitat member has an associated probability, which indicates the likelihood that it exists as a solution for a given problem. If this probability is very low then that solution is likely to mutate to some other solution. Similarly if the probability of some solution is higher then that solution has very little chance to mutate. Mutation rate of each set of solution can be calculated in terms of species count probability using the following equation:

$$m(S) = m_{max}\left(\frac{1 - P_s}{P_{max}}\right) \tag{22}$$

where, $m_{max}$ is a user-defined parameter. Details are available in [30],[31].

### C. BBO Algorithm for ORPF Problem

In the present work, the ORPF problem has been solved using BBO. The basic BBO [30] algorithm can handle several numbers of variables effectively. The basic control variables of an ORPF problem, which are represented by the *SIVs* of each habitat, are generator bus voltages, tap ratio of OLTC transformers and reactive power output of shunt compensators. Several *SIV* sets together form the habitat matrix [31].

*Initialization of the SIV:* Each element of the Habitat matrix i.e. each *SIV* of a given habitat set is initialized randomly within the effective operating limits. The initialization of the control variables are based on (9)-(12).

In the proposed BBO algorithm, the *SIVs* have been updated in a search space regardless of the variable type. The values of dependent variables are next computed using Newton−Raphson power flow [32], to determine their violations, if any, from the prescribed limits. The objective function value is next computed using (14). The algorithm to solve ORPF problems are given below:

*Step 1)* Read in the number of Generator units, number of tap changing transformers, number of shunt compensators. All these together define the size of *SIV* $m$ in BBO algorithm. Initialize no. of Habitat $H$, the BBO parameters like Habitat Modification Probability $P_{mod}$, Mutation Probability, maximum mutation rate $m_{max}$, maximum immigration rate $I$, maximum emigration rate $E$, step size for numerical integration $dt$ etc. Set maximum no. of iterations $Iter_{max}$ and no. of elite habitat $p$.

*Step 2)* Each *SIV* of a given habitat of $H$ matrix is initialized using the concept mentioned in "*Initialization of the SIV*". Each habitat represents a potential solution to the problem.

*Step 3)* Run the Newton−Raphson (NR) load flow program using these *SIVs* and determine the dependent variables of (5), to check whether they satisfy the inequality constraints of (10), and (13). If the values of dependent variables for any habitat set do not satisfy these constraints; then calculate the amount of violation of each dependent variable from their respective operating limits.

*Step 4)* Calculate the *HSI* (fitness value) for each habitat set of the total habitat set as per (14) for given emigration rate $\mu$, immigration rate $\lambda$. Here, *HSI* represents the active power loss.

*Step 5)* Based on the *HSI* value elite habitats are identified. Here elite term is used to indicate those habitat sets, which give best *HSI* values. Top $p$ habitat sets are kept as it is after individual iteration without making any modification on it.

*Step 6)* Migration operation is performed probabilistically on those *SIVs* of non-elite habitats, selected for migration as detailed in [30], [31].

*Step 7)* Species count probability of each habitat is updated using (18). Mutation operation is performed probabilistically on those non-elite habitats, selected for mutation as detailed in [30], [31].

*Step 8)* Go to *step 3* for the next iteration. This loop is terminated after a predefined number of iterations $Iter_{max}$ .

After each habitat is modified (*steps 6 and 7*), its feasibility as a problem solution should be verified. If the newly generated *SIVs* are feasible, then the dependent variables are executed using that *SIV* sets. A *SIV* set is feasible, if individual *SIV* and dependent variables satisfy different operational constraints of ORPF problem. If control variables (i.e. *SIVs*) are not feasible, the following method is implemented in order to map it to the set of feasible solutions.

Suppose, $U_i$ is the value of $i-th$ control variable of the ORPF problem, generated after migration and mutation operation. If $U_i^{max}$ and $U_i^{min}$ are the upper and lower operating limit of i−th control variable respectively, then Operating limit constraints are satisfied in the following manner:-

If output of $i-th$ control variable, $U_i > U_i^{max}$

$$U_i = U_i^{max}$$

end

If output of $i-th$ control variable, $U_i < U_i^{min}$

$$U_i < U_i^{min}$$

end

If output of $i-th$ control variable, $U_i$ is within its maximum and minimum operation limit

$$U_i = U_i$$

end

After fixing the control variables to their respective limits, dependent variables are re-determined using NR load flow method. If these dependent variables violate their respective operation limit constraints, calculate the amount of violation of each dependent variable from their respective operating limits and add these values in (14).

TABLE I
BEST CONTROL VARIABLES SETTINGS FOR IEEE 30-BUS SYSTEM (ACTIVE POWER LOSS MINIMIZATION)

| Control Variable setting (p.u.) | Active Power Loss (p.u.) | | | |
|---|---|---|---|---|
| | Base Case [33] | **BBO** | CLPSO [35] | PSO [35] |
| $V_1$ | 1.05 | 1.1000 | 1.1000 | 1.1000 |
| $V_2$ | 1.04 | 1.0944 | 1.1000 | 1.1000 |
| $V_5$ | 1.01 | 1.0749 | 1.0795 | 1.0867 |
| $V_8$ | 1.01 | 1.0768 | 1.1000 | 1.1000 |
| $V_{11}$ | 1.05 | 1.0999 | 1.1000 | 1.1000 |
| $V_{13}$ | 1.05 | 1.0999 | 1.1000 | 1.1000 |
| $T_{11}$ | 1.078 | 1.0435 | 0.9154 | 0.9587 |
| $T_{12}$ | 1.069 | 0.90117 | 0.9000 | 1.0543 |
| $T_{15}$ | 1.032 | 0.98244 | 0.9000 | 1.0024 |
| $T_{36}$ | 1.068 | 0.96918 | 0.9397 | 0.9755 |
| $Q_{c10}$ | 0.0 | 0.049998 | 0.049265 | 0.042803 |
| $Q_{c12}$ | 0.0 | 0.04987 | 0.050000 | 0.050000 |
| $Q_{c15}$ | 0.0 | 0.049906 | 0.050000 | 0.030288 |
| $Q_{c17}$ | 0.0 | 0.04997 | 0.050000 | 0.040365 |
| $Q_{c20}$ | 0.0 | 0.049901 | 0.050000 | 0.026697 |
| $Q_{c21}$ | 0.0 | 0.049946 | 0.050000 | 0.038894 |
| $Q_{c23}$ | 0.0 | 0.038753 | 0.050000 | 0.000000 |
| $Q_{c24}$ | 0.0 | 0.049867 | 0.050000 | 0.035879 |
| $Q_{c29}$ | 0.0 | 0.029098 | 0.050000 | 0.028415 |
| Active Power Loss (p.u.) | 0.05812 | 0.045511 | 0.045615 | 0.046282 |

TABLE II
BEST SOLUTIONS FOR ALL THE METHODS ON IEEE 30-BUS SYSTEM (P.U.)

| Algorithms | $\sum P_G$ | $P_{loss}$ | $P_{SAVE}\%$ |
|---|---|---|---|
| BBO | 2.879511 | 0.045511 | 21.69477 |
| CLPSO [35] | 2.879615 | 0.045615 | 21.51583 |
| PSO [35] | 2.880212 | 0.046282 | 20.36820 |

## IV. NUMERICAL EXAMPLES AND SIMULATION RESULTS

Proposed BBO algorithm has been applied for minimization of active power loss in two different test systems, viz., IEEE 30-bus test system [33] and IEEE 57-bus system [34].Programs have been written in MATLAB-7 language and executed on a 2.3 GHz Pentium IV personal computer with 512-MB RAM. After a number of careful experimentation, following optimum values of BBO parameters have finally been settled for all cases: Habitat size = 50, Habitat Modification Probability = 1, Immigration Probability bounds per gene = [0, 1], step size for numerical integration = 1, maximum immigration & emigration rate for each island = 1, number of elite habitat $p$ = 2 and Mutation Probability = 0.005.

### *A. Description of the Test Systems and Simulation Results*

The effectiveness of the BBO algorithm has been demonstrated through solution of ORPF problem in, IEEE 30-bus test system and IEEE 57-bus system.

TABLE III
COMPARISON OF EFFICACY AMONG DIFFERENT METHODS FOR IEEE 30-BUS SYSTEM AFTER 100 TRIALS (ACTIVE POWER LOSS MINIMIZATION)

| Methods | Active Power Loss (p.u.) | | | Simulation Time (Sec.) | Success Rate (%) |
|---|---|---|---|---|---|
| | Max. | Min. | Average | | |
| **BBO** | 0.045522 | 0.045511 | 0.045515 | 110 | 96 |
| PSO [35] | 0.047986 | 0.046282 | 0.047363 | 130 | 43 |
| CLPSO [35] | 0.046833 | 0.045615 | 0.046397 | 138 | 80 |

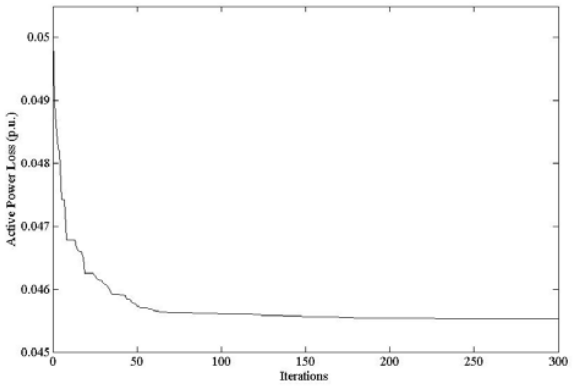


Fig. 2. Convergence Characteristic of IEEE 30-Bus system for Minimization of Loss

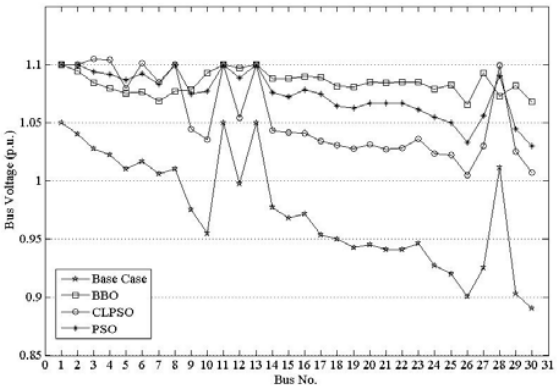


Fig. 3. Bus voltage profiles for different techniques on IEEE 30-Bus system

*1) IEEE* 30*-Bus Power System:* The line and bus data and the minimum and maximum limits on control variables and dependent variables have been adapted from [33]. The system has six generators at buses 1, 2, 5, 8, 11 and 13 and four transformers with off-nominal tap ratio in lines 6-9, 6-10, 4-12, and 28-27. In addition, shunt $VAR$ compensating devices are connected at bus bars 10, 12, 15, 17, 20, 21, 23, 24, and 29 for reactive power control as in [35]. The total power demand of the system is 2.834 p.u. on 100 MVA base. The voltages of all load bus and generator bus have been constrained within limits of 0.95 p.u. to 1.10 p.u. The optimum settings of the control variables for minimization of active power loss as obtained from proposed BBO, PSO [35] and comprehensive learning particle swarm optimizer (CLPSO) [35] have been presented in table I. From the table II, it is seen that BBO is able to reduce the active power loss, with respect to the base case, by 21.69477 % [33] whereas CLPSO [35] has reduced it by 21.51583%. The convergence characteristic is shown in figure 2. Figure 3 shows the voltage magnitudes of all the bus bars as calculated from the ORPF solution by the different methods. It can be seen that all the bus voltages obtained by the proposed method are within the limits. Further, the standard deviation of the bus voltages in case of BBO is 0.0093 p.u.; where as it is 0.0198 p.u., 0.034 p.u. and 0.0474 p.u. respectively in PSO, CLPSO and Base case. This implies that the BBO approach has done two jobs simultaneously. In one hand it has minimized active power loss and on the other hand it has improved voltage profile in a prominent manner than the other approaches employed on this test system. The minimum, maximum and average active power loss as obtained by BBO is presented in table III along with those using PSO [35] and CLPSO [35] over 100 trials. It may be seen that the results are favorable with BBO. Average simulation time of BBO, CLPSO [35] and PSO [35] are 110 sec., 138 sec. and 130 sec. respectively. Again BBO converges to minimum value 96 times out of 100 trials. Hence its success rate is 20% higher than CLPSO (80 times) [35]. Hence, it affirms that BBO is statistically more robust in global searching ability and computational efficiency.

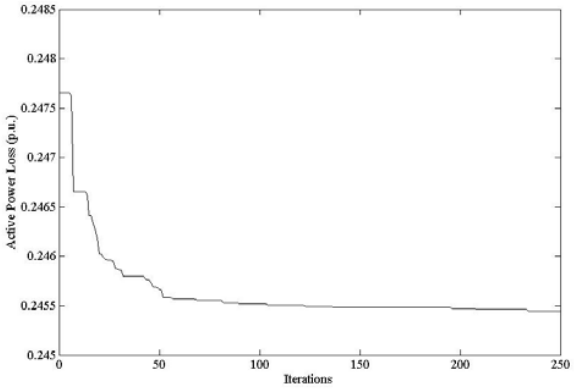


Fig. 4. Convergence Characteristic of IEEE 57-Bus system for Minimization of Loss (without relaxing Qlimit of Bus No. 2 and 9)

*2) IEEE* 57*-Bus Power System:* The standard IEEE 57-bus system consists of 80 transmission lines; seven generators at buses 1, 2, 3, 6, 8, 9, 12; and 15 OLTC transformers. The reactive power sources are considered at bus no. 18, 25 and 53. Line data, bus data and the minimum and maximum limits on control variables and dependent variables have been adapted from [34]. The total system active and reactive power demand are 12.508 p.u. and 3.364 p.u. on 100 MVA base. The voltages of all load bus and generator bus have been constrained within limits of 0.94 p.u. to 1.06 p.u. Active power loss along with control variable settings obtained from BBO, canonical genetic algorithm (CGA) [29], SOA [29], Local Search based self-adaptive differential evolution (L-SaDE) [29], SPSO [29], CLPSO [29], PSO with a constriction factor (PSO-cf) [29], PSO with adaptive inertia weight (PSO-w) [29] have been presented in table IV. The minimum active power loss obtained by BBO is 0.24544 p.u.. This is 2.773 % better than the results obtained by CGA [32], where there are no violation of any control and dependent variables limits in either method. Apparently the best result obtained by SOA [29] is a bit lower

TABLE IV
BEST CONTROL VARIABLES SETTINGS FOR IEEE 57-BUS SYSTEM (ACTIVE POWER LOSS MINIMIZATION)

| Control Variable setting | Active Power Loss (p.u.) | | | | | | | | |
|---|---|---|---|---|---|---|---|---|---|
| | CGA [29] | BBO | BBO (after relaxing Qlimt of Bus 2 and 9) | SOA [29] | L-SaDE [29] | SPSO-07 [29] | CLPSO [29] | PSO-cf [29] | PSO-w [29] |
| $V_1$ | 0.9686 | 1.0600 | 1.0600 | 1.0600 | 1.0600 | 1.0596 | 1.0541 | 1.0600 | 1.0600 |
| $V_2$ | 1.0493 | 1.0504 | 1.0580 | 1.0580 | 1.0574 | 1.0580 | 1.0529 | 1.0586 | 1.0578 |
| $V_3$ | 1.0567 | 1.0440 | 1.0442 | 1.0437 | 1.0438 | 1.0488 | 1.0337 | 1.0464 | 1.04378 |
| $V_6$ | 0.9877 | 1.0376 | 1.0364 | 1.0352 | 1.0364 | 1.0362 | 1.0313 | 1.0415 | 1.0356 |
| $V_8$ | 1.0223 | 1.0550 | 1.0567 | 1.0548 | 1.0537 | 1.0600 | 1.0496 | 1.0600 | 1.0546 |
| $V_9$ | 0.9918 | 1.0229 | 1.0377 | 1.0369 | 1.0366 | 1.0433 | 1.0302 | 1.0423 | 1.0369 |
| $V_{12}$ | 1.0044 | 1.0323 | 1.0351 | 1.0336 | 1.0323 | 1.0356 | 1.0342 | 1.0371 | 1.0334 |
| $T_{4-18}$ | 0.92 | 0.96693 | 0.99165 | 1.00 | 0.94 | 0.95 | 0.99 | 0.98 | 0.90 |
| $T_{4-18}$ | 0.92 | 0.99022 | 0.96447 | 0.96 | 1.00 | 0.99 | 0.98 | 0.98 | 1.02 |
| $T_{21-20}$ | 0.97 | 1.0120 | 1.0122 | 1.01 | 1.01 | 0.99 | 0.99 | 1.01 | 1.01 |
| $T_{24-26}$ | 0.90 | 1.0087 | 1.0110 | 1.01 | 1.01 | 1.02 | 1.01 | 1.01 | 1.01 |
| $T_{7-29}$ | 0.91 | 0.97074 | 0.97127 | 0.97 | 0.97 | 0.97 | 0.99 | 0.98 | 0.97 |
| $T_{34-32}$ | 1.10 | 0.96869 | 0.97227 | 0.97 | 0.97 | 0.96 | 0.93 | 0.97 | 0.97 |
| $T_{11-41}$ | 0.94 | 0.90082 | 0.90095 | 0.90 | 0.90 | 0.92 | 0.91 | 0.90 | 0.90 |
| $T_{15-45}$ | 0.95 | 0.96602 | 0.97063 | 0.97 | 0.97 | 0.96 | 0.97 | 0.97 | 0.97 |
| $T_{14-46}$ | 1.03 | 0.95079 | 0.95153 | 0.95 | 0.96 | 0.95 | 0.95 | 0.96 | 0.95 |
| $T_{10-51}$ | 1.09 | 0.96414 | 0.96252 | 0.96 | 0.96 | 0.97 | 0.98 | 0.97 | 0.96 |
| $T_{13-49}$ | 0.90 | 0.92462 | 0.92227 | 0.92 | 0.92 | 0.92 | 0.95 | 0.93 | 0.92 |
| $T_{11-43}$ | 0.90 | 0.95022 | 0.95988 | 0.96 | 0.96 | 1.00 | 0.95 | 0.97 | 0.96 |
| $T_{40-56}$ | 1.00 | 0.99666 | 1.0018 | 1.00 | 1.00 | 1.00 | 1.00 | 0.99 | 1.00 |
| $T_{39-57}$ | 0.96 | 0.96289 | 0.96567 | 0.96 | 0.96 | 0.95 | 0.96 | 0.96 | 0.96 |
| $T_{9-55}$ | 1.00 | 0.96001 | 0.97199 | 0.97 | 0.97 | 0.98 | 0.97 | 0.98 | 0.97 |
| $Q_{c18}$ | 0.084 | 0.09782 | 0.09640 | 0.09984 | 0.08112 | 0.03936 | 0.09888 | 0.09984 | 0.05136 |
| $Q_{c25}$ | 0.00816 | 0.058991 | 0.05897 | 0.05904 | 0.05808 | 0.05664 | 0.05424 | 0.05904 | 0.05904 |
| $Q_{c53}$ | 0.05376 | 0.6289 | 0.062948 | 0.06288 | 0.06192 | 0.03552 | 0.06288 | 0.06288 | 0.06288 |
| Active Power Loss (p.u.) | 0.2524411 | 0.24544 | 0.242616 | 0.2426548[1] | 0.2426739[2] | 0.2443043[3] | 0.2451520[4] | 0.2428022[5] | 0.2427052[6] |

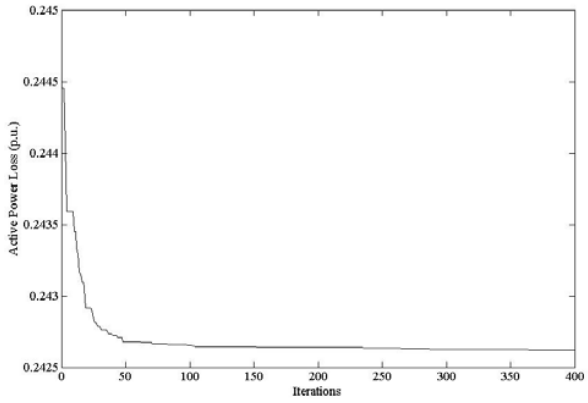


Fig. 5. Convergence Characteristic of IEEE 57-Bus system for Minimization of Loss (after relaxing Qlimit of Bus No. 2 and 9)

than BBO. However, for the control variable settings of SOA [29], L-SaDE [29], SPSO-07 [29], CLPSO [29], PSO-cf [29], PSO-w [29] the reactive power generation of bus number 2 and 9, on calculation comes much higher than their respective capacity constraints of 0.50 p.u. and 0.09 p.u. The details have been indicated in the foot-note of table IV. In, most of the cases, reactive power generation of bus number 2 and 9 have come nearer to 0.9 p.u. and 0.6 p.u. respectively. So the program was run again after increasing the reactive power generation capacity of these two buses to 0.9 p.u. and 0.6 p.u. This has reduced the active power loss to 0.242616 p.u., which is less than the best results by SOA [29].

Reduction in active power loss with respect to base case [29], as achieved by BBO and other techniques have been shown in table V. From the table it can be seen that active power loss has reduced by 13.7657 % when there is no violation of any constraint. This is 2.4598 % less than recently reported best result of CGA [29]. When reactive power limit of bus 2 and 9 is relaxed; power loss has reduced by 14.7579 %. This is 0.0136 % less than the best results of SOA [29].

From table VI, it can be seen that minimum, maximum and average active power loss obtained by BBO (for both the cases) over 30 runs are very close to other methods. Considering the relaxation of reactive power generation; minimum, maximum and average active power loss obtained are less than previously reported best results. For both the cases, BBO converges to optimum value 29 times and 27 times out of 30 trials. Its

[1]Infeasible solution as reactive power of generators at bus 2 and 9 for the schedule mentioned in [29] violates their limits by 75.20 % and 560.56 % respectively. Reactive power source at bus 25 also violates its maximum limit.

[2]Infeasible solution as reactive power of generators at bus 2 and 9 for the schedule mentioned in [29] violates their limits by 68.96 % and 594 % respectively. Also active power loss for the above mentioned schedule comes 0.2430 p.u., which is higher than reported in the literature [29].

[3]Infeasible solution as reactive power of generators at bus 2 and 9 for the schedule mentioned in [29] violates their limits by 65.88 % and 647.56 % respectively. Also voltage magnitude of Bus 29, 45 and 46 exceeds the upper limit of load Bus voltage 1.06.

[4]Infeasible solution as reactive power of generators at bus 2 and 9 for the schedule mentioned in [29] violates their limits by 93.94 % and 462.44 % respectively. Also voltage magnitude of Bus 43 is 1.0607 which exceeds the upper limit of load Bus voltage 1.06.

[5]Infeasible solution as reactive power of generators at bus 2 and 9 for the schedule mentioned in [29] violates their limits by 74.64 % and 598.67 % respectively.

[6]Infeasible solution as reactive power of generators at bus 2 and 9 for the schedule mentioned in [29] violates their limits by 73.02 % and 567.56 % respectively. Also voltage magnitude of Bus 45 and 55 exceeds the upper limit of load Bus voltage 1.06.

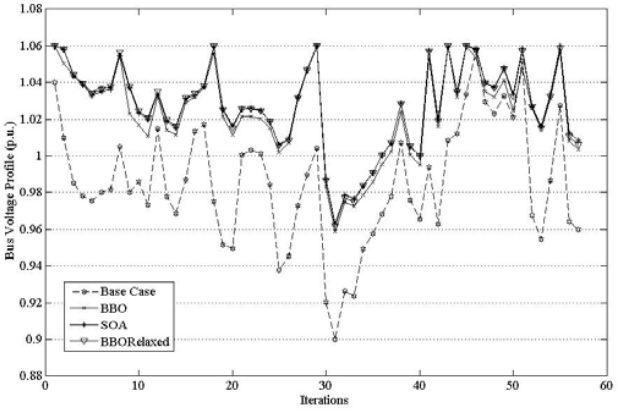


Fig. 6. Bus voltage profiles for different techniques on IEEE 57-Bus system

TABLE V
BEST SOLUTIONS FOR ALL THE METHODS ON IEEE 57-BUS SYSTEM (P.U.)

| Algorithms | $\sum P_G$ | $P_{loss}$ | $P_{SAVE}\%$ |
|---|---|---|---|
| BBO | 12.75344 | 0.24544 | 13.7657 |
| BBO (after relaxing Qlimt of Bus 2 and 9) | 12.750616 | 0.242616 | 14.7579 |
| CGA [29] | 12.7604 | 0.2524411 | 11.3059 |
| SOA [29] | 12.7507 | 0.2426548 | 14.7443 |
| L-SaDE [29] | 12.7507 | 0.2426739 | 14.7376 |
| SPSO-07 [29] | 12.7533 | 0.2443043 | 14.1647 |
| CLPSO [29] | 12.7531 | 0.2451520 | 13.8669 |
| PSO-cf [29] | 12.7508 | 0.2428022 | 14.6925 |
| PSO-w [29] | 12.7507 | 0.2427052 | 14.7266 |

success rate to reach optimum solution is 96.67 % and 90 % respectively. Hence, it reproduces global search ability of BBO.

The convergence characteristics using BBO for both the cases are shown in figure 4 and figure 5. From figure 6, it is observed that all the bus voltages optimized by BBO are within the limits of 0.94 p.u. to 1.06 p.u. But in case of CLPSO, PSO-w, PSO-cf voltages of few bus have crossed the specified limits [29]. Standard deviation of all bus voltages in case of BBO are 0.0244 p.u. (without relaxing reactive power limit) and 0.0229 (after relaxing reactive power limit); where as it is 0.0237 p.u., in case of SOA. Thus, both improvement in voltage profile and active power loss observed in case of BBO.

TABLE VI
COMPARISON OF EFFICACY AMONG DIFFERENT METHODS FOR IEEE 57-BUS SYSTEM AFTER 30 TRIALS (ACTIVE POWER LOSS MINIMIZATION)

| Methods | Active Power Loss (p.u.) | | | Average Simulation | Success |
|---|---|---|---|---|---|
| | Max. | Min. | Average | Time (Sec.) | Rate (%) |
| **BBO** | 0.245452 | 0.24544 | 0.245445 | 232.32 | 96.67 |
| BBO (after relaxing Qlimt of Bus 2 and 9) | 0.242621 | 0.242616 | 0.242619 | 332.15 | 90.00 |
| CGA [29] | 0.2750772 | 0.2524411 | 0.2629356 | 411.38 | NA* |
| SOA [29] | 0.2428046 | 0.2426548 | 0.2427078 | 391.32 | NA |
| L-SaDE [29] | 0.2439142 | 0.2426739 | 0.2431129 | 410.14 | NA |
| SPSO-07 [29] | 0.2545745 | 0.2443043 | 0.2475227 | 137.35 | NA |
| CLPSO [29] | 0.2478083 | 0.2451520 | 0.2467307 | 426.85 | NA |
| PSO-cf [29] | 0.2603275 | 0.2428022 | 0.2469805 | 408.19 | NA |
| PSO-w [29] | 0.2615279 | 0.2427052 | 0.2472596 | 408.48 | NA |

Average simulation time taken by BBO (both the cases) are 232.32 sec. and 332.15 sec.. This is 40.6317 % and 15.1206 % less than that of SOA [29].Therefore, improved computational efficiency of BBO is also prominent from these results.

## V. Conclusion

In this paper, the BBO has been successfully implemented to solve ORPF problems for minimization of active power loss. This approach has been tested and examined on both IEEE 30−bus and IEEE 57−bus systems to demonstrate its effectiveness. The results obtained from the BBO approach were compared to those reported in the recent literature. It has been observed here, that the BBO has the ability to reduce the active power loss reasonably without violating any constraints. When some constraints are relaxed like observed in recent literature, BBO is able to give better quality solution in comparison to the best results reported in recent recent literature. Moreover, BBO possesses excellent convergence characteristics and robustness compared to SOA, CLPSO and other techniques. Therefore, from the simulation results it may be concluded that the BBO is superior to the other algorithms in terms of solution quality, computational efficiency and robustness for solving ORPF problems.

## References

[1] S. S. Sachdeva and R. Billinton, Optimum network VAR planning by nonlinear programming. IEEE Trans. on Pwr. Apparatus and Syst. vol. PAS-92, no. 4, pp. 1217-1225, 1973.
[2] A.A. Abou El-Ela and M.A. Abido, "Optimal operation strategy for reactive power control Modeling", simulation and control, part A vol. 41, no. 3, AMSE Press, pp. 19-40, 1992.
[3] R. Mota-Palomino and V.H. Quintana, "Sparse reactive power scheduling by a penalty-function linear programming technique", IEEE Trans Pwr Syst , vol. 1, no. 3, pp. 31-39, 1986.
[4] V.H. Quintana, M. Satos-nieto, "Reactive power dispatch by successive quadratic programming", IEEE Trans.EnergyConvers.,vol.4,no3,pp.425-35, 89.
[5] M. R. Bjelogrlic, M. S. Calovic, B. S. Babic, et. al., "Application of Newton's optimal power flow in voltage/reactive power control", IEEE Trans Pwr Syst, vol. 5, no. 4, pp. 1447-1454, 1990.
[6] E. Rezania, S. M. Shahidehpour, "Real power loss minimization using interior point method", Int J Elec Pwr Energy Syst, vol.23,no.1,pp.45-56, 2001.
[7] Wei Yan, J. Yu, D. C. Yu and K. Bhattarai, "A new optimal reactive power flow model in rectangular form and its solution by predictor corrector primal dual interior point method", IEEE Trans. Pwr. Syst.,vol.21,no.1,pp.61-67, 2006.
[8] K. Aoki, M. Fan, A. Nishikori, "Optimal VAR planning by approximation method for recursive mixed-integer linear programming", IEEE Trans. on Pwr. Syst., vol. 3, no. 4, pp. 1741-1747, 1988.
[9] N. Deeb, S.M. Shahidehpour, Linear reactive power optimization in a large power network using the decomposition approach, IEEE Trans. on Pwr. Syst., vol. 5, no. 2, pp. 428-438, 1990.
[10] F.C. Lu, Y.Y. Hsu, "Reactive power/voltage control in a distribution substation using dynamic programming", IEE Proc. Gener., Transm. and Distrib., vol. 142, no. 6, pp. 639-645, 1995.
[11] K. Iba, "Reactive power optimization by genetic algorithm", IEEE Trans. on Pwr. Syst , vol. 9, no. 2, pp. 685-692, 1994.
[12] K.Y. Lee, Y.M. Park, Optimization method for reactive power planning by using a modified simple genetic algorithm, IEEE Trans. on Pwr. Syst, vol. 10, no. 4, pp. 1843-1850, 1995.
[13] Q. H. Wu, Y. J. Cao, and J. Y. Wen, "Optimal reactive power dispatch using an adaptive genetic algorithm," Int. J. Elect. Power Energy Syst., vol. 20, pp. 563-569, Aug. 1998.

[14] G. A. Bakare, G. K. Venayagamoorthy, and U. O. Aliyu, "Reactive power and voltage control of the Nigerian grid system using microgenetic algorithm," in Proc. IEEE Power Eng. Soc. General Meeting, vol. 2, pp. 1916-1922, San Francisco, CA, 2005.
[15] W. Yan, F. Liu, C.Y. Chung, K.P. Wong, "A hybrid genetic algorithm-interior point method for optimal reactive power flow", IEEE Trans. on Pwr. Syst., vol. 21, no. 3, pp. 1163-1169, 2006.
[16] Q.H. Wu, J.T. Ma, "Power system optimal reactive power dispatch using evolutionary programming", IEEE Trans. on Pwr. Syst., vol. 10, no. 3, pp. 1243-1249, 1995.
[17] L.L. Lai, J.T. Ma, "Application of evolutionary programming to reactive power planning-comparison with nonlinear programming approach", IEEE Trans. on Pwr. Syst., vol. 12, no. 1, pp. 198-206, 1997.
[18] H. Yoshida et al., "A particle swarm optimization for reactive power and voltage control considering voltage security assessment," IEEE Trans. Power Syst., vol. 15, no. 4, pp. 1232-1239, Nov. 2001.
[19] W. Zhang, Y. Liu, and M. Clerc, "An adaptive PSO algorithm for reactive power optimization," in Proc. 6th Int. Conf. Advance in Power System Control, Operatation and Management, Hong Kong, Nov. 2003, pp. 302-307.
[20] B. Zhao, C. X. Guo, and Y. J. Cao, "A multi-agent based particle swarm optimization approach for reactive power dispatch," IEEE Trans. Pwr. Syst., vol. 20, no. 2, pp. 1070-1078, May 2005.
[21] A. A. A. Esmin, G. Lambert-Torres, and A. C. Zambroni de Souza, "A hybrid particle swarm optimization applied to loss power minimization," IEEE Trans. Power Syst., vol. 20, no. 2, pp. 859-866, May 2005.
[22] M. S. Kumari and M. Sydulu, "Improved particle swarm algorithm applied to optimal reactive power control," in Proc. IEEE Int. Conf. Industrial Technology, 2006, pp. 1873-1878.
[23] J. G. Vlachogiannis and K. Y. Lee, "A comparative study on particle swarm optimization for optimal steady-state performance of power systems," IEEE Trans. Power Syst., vol. 21, no. 4, pp. 1718-1728, Nov. 2006.
[24] G. Cai, Z. Ren, and T. Yu, "Optimal reactive power dispatch based on modified particle swarm optimization considering voltage stability in Proc. IEEE Power Eng. Soc. General Meeting, 2007, pp. 1-5.
[25] C. H. Liang, C.Y. Chung, K. P. Wong, X. Z. Duan, C. T. Tse, "Study of differential evolution for reactive power flow", IET Proc. Gener. Transm. Distrib., vol. 1, no. 2, pp. 253-260, 2007.
[26] G. A. Bakare, G. Krost, G. K.Venayagamoorthy, U. O. Aliyu, "Differential evolution approach for reactive power optimization of Nigerian grid system," in Proc. IEEE Power Eng. Soc. General Meeting, Tampa, FL, pp. 1-6, Jun. 24-28 2007.
[27] M. Varadarajan, K. S. Swarup, "Network loss minimization with voltage security using differential evolution",Elect.Pwr Syst.Res.,vol.78,pp.815-23, 08.
[28] C. Y. Chung, C. H. Liang, K. P. Wong, X. Z. Duan, "Hybrid algorithm for differential evolution and evolutionary programming for optimal ractive power flow", IET Proc. Gener., Transm. & Distrib., vol. 4, no. 1, pp. 84-93, 2010.
[29] C. Dai, W. Chen, "Seeker Optimization Algorithm for Optimal Reactive Power Dispatch", IEEE Trans. Power Syst., vol. 24, no. 3, pp. 1218-31, 2009.
[30] Dan Simon, "Biogeography-Based Optimization", IEEE Transaction on Evolutionary Computation, vol. 12, no. 6, pp. 702-713, December 2008.
[31] Bhattacharya A., Chattopadhyay P.K., "Biogeography-Based Optimization for Different Economic Load Dispatch Problems", IEEE Trans. on Power Syst., vol. 25, no. 2, pp. 1064-1075, May 2010.
[32] Tinney, W.F., Hart, C.E., "Power Flow Solution by Newton's Method", IEEE Trans. on Pwr Apparatus and Syst., vol.PAS-86,no.11,pp. 1449-60, 1967.
[33] K. Lee, Y. Park and J. Ortiz, "A united approach to optimal real and reactive power dispatch", IEEE Trans Pwr Appar Syst vol. PAS-104, no. 5, pp. 1147-1153, 1985.
[34] The IEEE 57-Bus Test System, Available online: http://www.ee.washington.edu/research/pstca/ .
[35] K. Mahadevan, P. S. Kannan, "Comprehensive learning Particle Swarm Optimization for Reactive Power Dispatch," Int. J. Applied Soft Computing, vol. 10, no. 2, pp. 641-652, March 2010.

**Aniruddha Bhattacharya (M'09)** received the B.Sc. Engg. Degree in electrical engineering from the Regional Institute of Technology, Jamshedpur, India; in 2000 and the M.E.E. degree in electrical power system from Jadavpur University, Kolkata, India; in 2008. He is currently pursuing the Ph.D. degree as Senior Research Fellow in the Department of Electrical Engineering at Jadavpur University.

His employment experience includes the Siemens Metering Limited, India; Jindal Steel & Power Limited, Raigarh, India; Bankura Unnyani Institute of Engineering, Bankura, India and Dr. B. C. Roy Engineering College, Durgapur, India. His areas of interest include power system load flow, optimal power flow, economic load dispatch, and soft computing applications to different power system problems.

**Pranab Kumar Chattopadhyay** received the M.E.E degree in electrical power system from Jadavpur University, Kolkata, India, in 1971. He is currently working as a Professor in the Department of Electrical Engineering, Jadavpur University. His areas of interest include application of soft computing techniques to different power system problems.